JJMIE

Volume 16, Number 3, June. 2022
ISSN 1995-6665
Pages 369 – 379

Jordan Journal of Mechanical and Industrial Engineering

Torsional vibration of a Rod Composed of Two Dissimilar Frictionally Welded Parts with and without Crack in a Thermal Environment

Ahmed A. Ahmed[1*], Mohammadtaher M. Saeed Mulapeer [2]

[1]Chemical and Petrochemical Engineering Department, College of Engineering, Salahaddin University-Erbil, Erbil, 44001, Iraq

[2]Mechanical and Mechatronics Department, College of Engineering, Salahaddin University-Erbil, Erbil, 44001, Iraq

Received 4 Jan 2022 Accepted 27 Mar 2022

Abstract

In this study, a three-dimensional thermal environment effect in the form of thermal stresses on linear torsional vibration of non-cracked and cracked rods composed of two dissimilar rods welded by friction welding is investigated. The nonlinear Green strain relation is used to drive the nonlinear strains. Hamilton’s principle is used to drive equation of motion and corresponding boundary conditions. To model the crack, a torsional spring is used at the crack location. The crack is assumed to locate at the contact surface of the dissimilar welded rods. Effects of the thermal stresses in the form of the high temperature changes, crack depth ratio, and boundary conditions are examined on the torsional frequencies. Increasing the crack depth ratio at high temperatures results in a high reduction of the torsional frequencies.

Keywords: Thermal stresses; Torsional vibration; Cracked rod; Friction welding.

1. Introduction

Friction welding is one of the most important welding methods which is capable of welding similar and dissimilar parts to each other. In this welding type, one of the bodies, generally with a circular cross-section, turns with a constant rotational velocity, and the other body fixed in one head is pushed toward the turning body to be welded with it through the heat generated due to friction force between two surfaces in contact. The bodies or shafts that are welded by the friction welding method can have the same[1, 2] or different[3] cross-sectional areas in the surfaces which are in contact and must be welded. It has been observed that an interlayer piece such as a plate is used between two rods to increase the quality of the friction welding as performed by Hynes and Velu [4]. The thermal model for heat flow in a friction welding process is investigated by [5]. Generally, the pieces such as shafts or rods which are welded by friction rotary welding, contain some defects such as cracks. The cracks are the most common defects found in such structures which can be generated by mechanical stresses or/and thermal stresses arising from the dissimilarity of thermal expansion coefficients in the contact zone. The cracks are sometimes very dangerous especially if they are open crack types that are capable of propagating through the surface of a body. When a piece such as a shaft, rod, or beam is vibrating, the presence of the crack leads to a fatigue failure and decreases the lifetime. There are several methods to model the crack, such as modelling it with one or more springs, or directly driving the local flexibility induced by the crack to the pieces[6-11].

Several investigations have been devoted to study the torsional, axial, lateral, and coupled vibrations of different parts, such as plates, rods, and beams with and without crack effects. Nacy et al. [12]investigated the vibration analysis of the plates with spot welded stiffeners. Ghadiri et al. [13] studied the free vibration of an axially preloaded laminated composite beam carrying a spring-mass-damper system with a non-ideal support. Kachapi[14] presented the nonlinear vibration and frequency analysis of functionally graded-piezoelectric cylindrical nano-shell with surface elasticity. Abdullah et al. used nonlinear strains to find three-dimensional thermal stress effects on the linear[15]and nonlinear [16] torsional frequencies of the rods with different boundary conditions. Zhu and Li [17] investigated the longitudinal and torsional vibration of size-dependent rods using nonlocal integral elasticity. Li and Hu[18] studied the torsional vibration of bi-directional functionally graded nanotubes based on nonlocal theory.Barretta et al. [19]presented the stress-driven two-phase integral elasticity for torsion of nano-beams.

The crack effect is mostly demonstrated by its position and depth. The crack position and depth can highly impress the different behaviours such as the static and dynamic of the cracked bodies. The crack severity relates to the crack depth. This relation for the transverse crack differs from that of the axial, circumferential, or radial cracks. Dimarogonas and Massouros[20] presented a relation to determine the local flexibility or compliance added by the presence of a circumferential crack. In another investigation devoted to the sensitivity of the

* Corresponding author e-mail: ahmed.ahmed3@su.edu.krd.

structures such as rotors and shafts to cracks, a different relation was presented by Chondros and Dimarogonas[21] for the dimensionless flexibility of the cracked shaft. For a transverse crack, the relations for the local flexibility and dimensionless flexibility of a cracked beam were presented by Rizos et al.[22]. Loya et al. [23] presented the compatibility relations at the cracked location for a cracked rod in nanoscale for investigating the torsional frequencies. Marin [24] presented the domain of influence in thermoelasticity of bodies with voids. Marin [25] investigated a temporally evolutionary equation in elasticity of micropolar bodies with voids. Amini and Amiri [26]studied the ultrasonic vibration effects on friction stir welding process.

Based on the investigations mentioned above, an absence of studying the torsional vibration of a cracked rod composed of two dissimilar welded rods under the effect of the thermal stresses,is evident. This is the reason that this paper aims to develop a reliable and accurate mathematical model to evoke the behaviour of a frictionally welded rod under a torsional vibration. The equation takes into account the different stiffness of the rod sections and, consequently, a new computability equation at the crack location is obtained.It can be stated that the main purpose of this study is to determine how much the crack and three-dimensional thermal stresses can alter the torsional frequencies of a rod composed of two frictionally-welded parts.To enter the effects of the three-dimensional thermal stresses to the torsional equation of motion of the rod, the nonlinear strains must be obtained using the Green strain relation.

2. Theory

For a rod composed of two welded rods, a displacement field given by Eq. (1) can be defined.

$$u_x = 0, u_y = -z\phi(x,t), u_z = y\phi(x,t). \quad (1)$$

The displacement u_x, u_y, and u_z are, respectively, the displacements in x, y, and z directions. The transverse displacements $u_y$and u_z relate with the twisting angle $\phi(x,t)$. The nonlinear Green-Lagrange strain relation [27-29] is given by

$$\varepsilon_{ij} = \frac{1}{2}\left(\frac{\partial u_i}{\partial x_j} + \frac{\partial u_j}{\partial x_i} + \frac{\partial u_k}{\partial x_i}\frac{\partial u_k}{\partial x_j}\right). \quad (2)$$

The strains generated by mechanical stresses, can be obtained by substituting Eq. (1) into Eq. (2) as

$$\varepsilon_{xx} = \frac{1}{2}(y^2+z^2)\left(\frac{\partial\phi}{\partial x}\right)^2 = \frac{1}{2}r^2\left(\frac{\partial\phi}{\partial x}\right)^2, \varepsilon_{yy} = \varepsilon_{zz} = \frac{1}{2}\phi^2,$$
$$\varepsilon_{xy} = \varepsilon_{yx} = \frac{1}{2}\left(y\phi\frac{\partial\phi}{\partial x} - z\frac{\partial\phi}{\partial x}\right), \varepsilon_{zx} = \varepsilon_{xz} = \frac{1}{2}\left(y\frac{\partial\phi}{\partial x} + z\phi\frac{\partial\phi}{\partial x}\right), \varepsilon_{yz} = \varepsilon_{zy} = 0. \quad (3)$$

In this paper, the stiffness matrix of the isotropic material is used to obtain the stresses from the strains, because both welded segments of a rod are assumed to be isotropic materials. Using the stiffness matrix of the isotropic material and strains presented in Eq. (3), the corresponding stresses are determined as follows. The significance of the component of the stiffness matrix $[C_{ij}]$ is to relate the strains to stresses in one, two, or three dimensional problems. These components or coefficients are given for an isotropic material in Eq. (5).

$$\sigma_{xx} = C_{11}\varepsilon_{xx} + C_{12}\varepsilon_{yy} + C_{13}\varepsilon_{zz} = \frac{1}{2}r^2C_{11}\left(\frac{\partial\phi}{\partial x}\right)^2 + C_{12}\phi^2,$$
$$\sigma_{yy} = C_{21}\varepsilon_{xx} + C_{22}\varepsilon_{yy} + C_{23}\varepsilon_{zz} = \frac{1}{2}r^2C_{12}\left(\frac{\partial\phi}{\partial x}\right)^2 + \frac{1}{2}(C_{22}+C_{23})\phi^2,$$
$$\sigma_{zz} = C_{31}\varepsilon_{xx} + C_{32}\varepsilon_{yy} + C_{33}\varepsilon_{zz} = \frac{1}{2}r^2C_{12}\left(\frac{\partial\phi}{\partial x}\right)^2 + \frac{1}{2}(C_{22}+C_{23})\phi^2, \sigma_{xy} = 2C_{66}\varepsilon_{xy} = G\gamma_{xy} = G\left(y\phi\frac{\partial\phi}{\partial x} - z\frac{\partial\phi}{\partial x}\right), \sigma_{xz} = 2C_{55}\varepsilon_{xz} = G\gamma_{xz} = G\left(y\frac{\partial\phi}{\partial x} + z\phi\frac{\partial\phi}{\partial x}\right),$$
$$\sigma_{yz} = 0. \quad (4)$$

A crack can be modelled as a torsional spring whose stiffness is exactly the crack severity. Mathematical modeling of the crack will be more discussed in the incoming subsection. Fig. 1 shows a rod composed of two dissimilar segments with a crack located at the contact zone of the welded segments (distance b from the left end) under σ_{xx}^T, σ_{yy}^T, and σ_{zz}^T thermal stresses applied, respectively, in x, y, and z directions. Geometries and material properties of each segment of the rod can be similar or different.

Using the stiffness matrix of an isotropic rod $[C_{ij}]$ shown in Eq. (5), the relation between mechanical (σ_{ij}) and thermal stresses (σ_{ij}^T) and corresponding strains is written according to [15, 29-31]

$$\begin{Bmatrix} \sigma_{xx}+\sigma_{xx}^T \\ \sigma_{yy}+\sigma_{yy}^T \\ \sigma_{zz}+\sigma_{zz}^T \\ \sigma_{yz}+\sigma_{yz}^T \\ \sigma_{xy}+\sigma_{xy}^T \\ \sigma_{zx}+\sigma_{zx}^T \end{Bmatrix} = \begin{bmatrix} C_{11} & C_{12} & C_{13} & 0 & 0 & 0 \\ C_{21} & C_{22} & C_{23} & 0 & 0 & 0 \\ C_{31} & C_{32} & C_{33} & 0 & 0 & 0 \\ 0 & 0 & 0 & C_{44} & 0 & 0 \\ 0 & 0 & 0 & 0 & C_{55} & 0 \\ 0 & 0 & 0 & 0 & 0 & C_{66} \end{bmatrix} = \begin{Bmatrix} \varepsilon_{xx}-\alpha_x\Delta T \\ \varepsilon_{yy}-\alpha_y\Delta T \\ \varepsilon_{zz}-\alpha_z\Delta T \\ 2\varepsilon_{yz} \\ 2\varepsilon_{xy} \\ 2\varepsilon_{zx} \end{Bmatrix}. \quad (5)$$

$$C_{11} = C_{22} = C_{33} = \lambda + 2G, C_{12} = C_{13} = C_{23} = \lambda, C_{44} = C_{55} = C_{66} = G, \lambda = \frac{E\,v}{(1+v)(1-2v)}, G = \frac{E}{2(1+v)}, C_{ij} = C_{ji}. \quad (6)$$

$$\sigma_{xx}^T = -\left(C_{11}\alpha_x\Delta T + C_{12}\alpha_y\Delta T + C_{13}\alpha_z\Delta T\right),$$
$$\sigma_{yy}^T = -\left(C_{21}\alpha_x\Delta T + C_{22}\alpha_y\Delta T + C_{23}\alpha_z\Delta T\right),$$
$$\sigma_{zz}^T = -\left(C_{31}\alpha_x\Delta T + C_{32}\alpha_y\Delta T + C_{33}\alpha_z\Delta T\right), \alpha = \alpha_x = \alpha_y = \alpha_z, \Delta T = T - T_{room}. \quad (7)$$

For the isotropic materials, the thermal expansion in x, y, and z directions which are, respectively, denoted by α_x, α_y, and α_z are the same, and all of them are denoted byα.ExpressionΔT is temperature changes in which T_{room} is room temperature (stress-free temperature) and is assumed to be $298\,K$ or 25℃ and T is temperature of the rod.

In this study, boundary conditions and the torsional equation of motion are obtained using Hamilton's principle.

$$\int_0^t \delta(-K_E + U_s + U_T)\,dt = 0. \quad (8)$$

where K_E, U_s, and U_T are the kinetic energy, strain energy, and potential due to the thermal stresses.

Taking the variations of the$U_s$andK_E, the following relations are obtained.

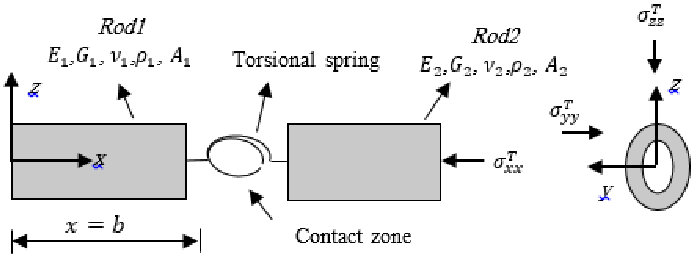

Figure 1. A cracked rod composed of two welded different rods under thermal stresses

$$\delta U_s = \delta \int_V \frac{1}{2}\left(\sigma_{xx}\varepsilon_{xx} + \sigma_{yy}\varepsilon_{yy} + \sigma_{zz}\varepsilon_{zz} + \sigma_{xy}\gamma_{xy} + \sigma_{xz}\gamma_{xz}\right) dV = \delta U_1 + \delta U_2 + \delta U_3 + \delta U_4 + \delta U_5 = \int_A dA\left\{\int_0^L\left[\frac{-3}{2}r^4C_{11}\left(\frac{\partial\phi}{\partial x}\right)^2\frac{\partial^2\phi}{\partial x^2} - r^2C_{12}\phi\left(\frac{\partial\phi}{\partial x}\right)^2 - r^2C_{12}\phi^2\frac{\partial^2\phi}{\partial x^2} + (C_{22}+C_{23})\phi^3 - Gr^2\frac{\partial^2\phi}{\partial x^2} - Gr^2\phi\left(\frac{\partial\phi}{\partial x}\right)^2 - Gr^2\phi^2\frac{\partial^2\phi}{\partial x^2}\right]\delta\phi dx + \left[\left(\frac{1}{2}r^4C_{11}\left(\frac{\partial\phi}{\partial x}\right)^3 + r^2C_{12}\phi^2\frac{\partial\phi}{\partial x} + Gr^2\frac{\partial\phi}{\partial x} + Gr^2\phi^2\frac{\partial\phi}{\partial x}\right)\delta\phi\right]_0^L\right\},$$

$$\delta U_1 = \delta\int_V \frac{1}{2}(\sigma_{xx}\varepsilon_{xx})\,dV, \quad \delta U_2 = \delta\int_V \frac{1}{2}(\sigma_{yy}\varepsilon_{yy})\,dV, \quad \delta U_3 = \delta\int_V \frac{1}{2}(\sigma_{zz}\varepsilon_{zz})\,dV, \quad \delta U_4 = \delta\int_V \frac{1}{2}(\sigma_{xy}\gamma_{xy})\,dV, \quad \delta U_5 = \delta\int_V \frac{1}{2}(\sigma_{xz}\gamma_{xz})\,dV.$$

$$\delta U_1 = \int_A dA\left\{\int_0^L\left[\frac{-3}{2}r^4C_{11}\left(\frac{\partial\phi}{\partial x}\right)^2\frac{\partial^2\phi}{\partial x^2} - \frac{1}{2}r^2C_{12}\phi\left(\frac{\partial\phi}{\partial x}\right)^2 - \frac{1}{2}r^2C_{12}\phi^2\frac{\partial^2\phi}{\partial x^2}\right]\delta\phi\,dx + \left[\left(\frac{1}{2}r^4C_{11}\left(\frac{\partial\phi}{\partial x}\right)^3 + \frac{1}{2}r^2C_{12}\phi^2\frac{\partial\phi}{\partial x}\right)\delta\phi\right]_0^L\right\}; \tag{9}$$

$$\delta U_2 = \delta U_3 = \int_A dA\left\{\int_0^L\left[\frac{-1}{4}r^2C_{12}\phi\left(\frac{\partial\phi}{\partial x}\right)^2 - \frac{1}{4}r^2C_{12}\phi^2\frac{\partial^2\phi}{\partial x^2} + \frac{1}{2}(C_{22}+C_{22})\phi^3\right]\delta\phi\,dx + \left[\left(\frac{1}{4}r^2C_{12}\phi^2\frac{\partial\phi}{\partial x}\right)\delta\phi\right]_0^L\right\},$$

$$\delta U_4 = \int_A dA\left\{\int_0^L G\left[-y^2\phi\left(\frac{\partial\phi}{\partial x}\right)^2 + yz\left(\frac{\partial\phi}{\partial x}\right)^2 - y^2\phi^2\frac{\partial^2\phi}{\partial x^2} + 2yz\phi\frac{\partial^2\phi}{\partial x^2} - z^2\frac{\partial^2\phi}{\partial x^2}\right]\delta\phi\,dx + \left[G\left(y^2\phi^2\frac{\partial\phi}{\partial x} - 2yz\phi\frac{\partial\phi}{\partial x} + z^2\frac{\partial\phi}{\partial x}\right)\delta\phi\right]_0^L\right\},$$

$$\delta U_5 = \int_A dA\left\{\int_0^L G\left[-y^2\frac{\partial^2\phi}{\partial x^2} - yz\left(\frac{\partial\phi}{\partial x}\right)^2 - z^2\phi^2\frac{\partial^2\phi}{\partial x^2} - 2yz\phi\frac{\partial^2\phi}{\partial x^2} - z^2\phi\left(\frac{\partial\phi}{\partial x}\right)^2\right]\delta\phi\,dx + \left[G\left(y^2\frac{\partial\phi}{\partial x} + 2yz\phi\frac{\partial\phi}{\partial x} + z^2\phi^2\frac{\partial\phi}{\partial x}\right)\delta\phi\right]_0^L\right\}.$$

$$\delta K_E = \delta\int_V \frac{\rho}{2}\left[\left(\frac{\partial u_x}{\partial t}\right)^2 + \left(\frac{\partial u_y}{\partial t}\right)^2 + \left(\frac{\partial u_z}{\partial t}\right)^2\right]dV = \int_0^L\int_0^R 2\rho\pi\, r^3dr\frac{\partial\phi}{\partial t}\left(\frac{\partial\delta\phi}{\partial t}\right) = \int_0^L S\frac{\partial\phi}{\partial t}\left(\frac{\partial\delta\phi}{\partial t}\right)dx,$$

$$\Rightarrow \int_0^t \delta K_E\,dt = \int_0^t\left[\int_0^L S\frac{\partial\phi}{\partial t}\left(\frac{\partial\delta\phi}{\partial t}\right)dx\right]dt = \int_0^L\left[\int_0^t S\frac{\partial\phi}{\partial t}\left(\frac{\partial\delta\phi}{\partial t}\right)dt\right]dx = \int_0^L\left[\left[S\frac{\partial\phi}{\partial t}\delta\phi\right]_0^t - \int_0^t S\frac{\partial^2\phi}{\partial t^2}\delta\phi dt\right]dx = \int_0^L\left[0 - \int_0^t S\frac{\partial^2\phi}{\partial t^2}\delta\phi dt\right]dx = \int_0^t\left[\int_0^L -S\frac{\partial^2\phi}{\partial t^2}\delta\phi dx\right]dt. \tag{10}$$

Praveen and Reddy [32]stated that the variation of the potential energy due to thermal stressesδU_T is given by

$$\delta U_T = \int_V \left(\sigma_{xx}^T\delta\varepsilon_{xx} + \sigma_{yy}^T\delta\varepsilon_{yy} + \sigma_{zz}^T\delta\varepsilon_{zz}\right)dV = \int_0^L\left[-\sigma_{xx}^T I_P\frac{\partial^2\phi}{\partial x^2} + \left(\sigma_{yy}^T + \sigma_{zz}^T\right)A\phi\right]\delta\phi\,dx + \left[\left(\sigma_{xx}^T I_P\frac{\partial\phi}{\partial x}\right)\delta\phi\right]_0^L. \tag{11}$$

Nonlinear torsional equation of motion and corresponding boundary conditions are obtained by substituting Eqs. (9) - (11) into Eq. (8),

$$\int_0^t\left[\left(Q_1\left(\frac{\partial\phi}{\partial x}\right)^3 + (Q_2+Q_4)\phi^2\frac{\partial\phi}{\partial x} + (Q_4+Q_x^T)\frac{\partial\phi}{\partial x}\right)\delta\phi\right]_0^L dt + \int_0^t\int_0^L\left[-3Q_1\left(\frac{\partial\phi}{\partial x}\right)^2\frac{\partial^2\phi}{\partial x^2} + (-Q_2 - Q_4)\phi\left(\frac{\partial\phi}{\partial x}\right)^2 + (-Q_2-Q_4)\phi^2\frac{\partial^2\phi}{\partial x^2} + Q_3\phi^3 + S\frac{\partial^2\phi}{\partial t^2} - Q_4\frac{\partial^2\phi}{\partial x^2} - Q_x^T\frac{\partial^2\phi}{\partial x^2} + \left(Q_y^T + Q_z^T\right)\phi\right]\delta\phi\,dx\,dt = 0. \tag{12}$$

$$\int_A dA = \int_0^R 2\pi r\,dr, r^2 = y^2 + z^2, I_P = \frac{\pi}{2}R^4, Q_1 = \int_A \frac{r^4}{2}C_{11}dA = C_{11}\frac{\pi}{6}R^6, Q_2 = \int_A r^2C_{12}dA = C_{12}I_P, Q_3 = \int_A (C_{22}+C_{23})dA = (C_{22}+C_{23})A, Q_4 = \int_A Gr^2dA = GI_P, S = \int_A 2\pi\rho\, r^3dr = \rho I_P, Q_x^T = \int_A r^2\sigma_{xx}^{Th}\,dA = \sigma_{xx}^T I_P, Q_y^T = \int_A \sigma_{yy}^{Th}\,dA = \sigma_{yy}^T A, Q_z^T = \int_A \sigma_{zz}^{Th}\,dA = \sigma_{zz}^T A. \tag{13}$$

Here,A is the cross-sectional area, I_P is the polar moment of inertia,R is the radius of the rod, andρ is the density. From Eq. (12) and using the expressions defined in Eq.(13), the equation of motion is obtained as

$$-C_{11}\frac{\pi}{2}R^6\left(\frac{\partial\phi}{\partial x}\right)^2\frac{\partial^2\phi}{\partial x^2} + (-C_{12}I_P - GI_P)\phi\left(\frac{\partial\phi}{\partial x}\right)^2 + (-C_{12}I_P - GI_P)\phi^2\frac{\partial^2\phi}{\partial x^2} + (C_{22}+C_{23})A\phi^3 + \rho I_P\frac{\partial^2\phi}{\partial t^2} - GI_P\frac{\partial^2\phi}{\partial x^2} - \sigma_{xx}^T I_P\frac{\partial^2\phi}{\partial x^2} + \left(\sigma_{yy}^T + \sigma_{zz}^T\right)A\phi = 0. \tag{14}$$

The torsional equation of motion given by Eq. (14) is a nonlinear equation including linear and nonlinear terms. Because in this study, the linear torsional frequencies will be investigated, the nonlinear terms of the equation of motion and boundary conditions will be neglected and finally, the linear equation of motion and corresponding boundary conditions will be presented in the following form as

$$-GI_P\frac{\partial^2\phi}{\partial x^2}-\sigma_{xx}^T I_P\frac{\partial^2\phi}{\partial x^2}+\left(\sigma_{yy}^T+\sigma_{zz}^T\right)A\phi-\rho I_P\frac{\partial^2\phi}{\partial t^2}=0. \quad (15)$$

$$\left[\left(GI_P\frac{\partial\phi}{\partial x}+\sigma_{xx}^T I_P\frac{\partial\phi}{\partial x}\right)\delta\phi\right]_0^L=0. \quad (16)$$

The equation of motion can be written in a more convenient manner as

$$g_1\frac{\partial^2\phi}{\partial x^2}+g_2\phi+g_3\frac{\partial^2\phi}{\partial t^2}=0. \quad (17)$$

$$\frac{\partial^2\phi}{\partial x^2}+P\phi+F\frac{\partial^2\phi}{\partial t^2}=0. \quad (18)$$

$$g_1=\left(-1-\frac{\sigma_{xx}^T}{G}\right),\quad g_2=\left(\frac{\sigma_{yy}^T+\sigma_{zz}^T}{GI_P}\right)A,\quad g_3=\frac{\rho}{G},\quad P=\frac{g_2}{g_1},\quad F=\frac{g_3}{g_1}. \quad (19)$$

2.1. racked rod equations

Generally, it is assumed that a crack divides the rod into two segments. If the rod is composed of two dissimilar smaller rods welded by friction welding, there will probably exist a crack or more at the welded or contact zone. So, it is assumed that the crack is located at $x=b=L_1$ which is exactly the end of the first segment as already shown in Fig. 1. It is worth mentioning that the total rod length is $L=L_1+L_2$ in which $L_1$is the length of the first segment of the rod and L_2 is the second segment length. One of the best methods for modelling the cracks is using the spring model. In this modeling, a spring or more is assumed to behave as a crack at the crack location whose stiffness relates with the crack severity. As the crack depth increases, the crack severity increases, and its effect increases. The crack results in additional flexibility which is known as local flexibility or compliance C. Equation of motion can be written according to Eq. (18) for each segment of the cracked rod as following in which $\phi_1(x,t)$, and $\phi_2(x,t)$ are twisting angles of the left and right segments.

$$\frac{\partial^2\phi_1}{\partial x^2}+P_1\phi_1+F_1\frac{\partial^2\phi_1}{\partial t^2}=0. \quad (20)$$

$$\frac{\partial^2\phi_2}{\partial x^2}+P_2\phi_2+F_2\frac{\partial^2\phi_2}{\partial t^2}=0. \quad (21)$$

$$g_{1,1}=\left(-1-\frac{\sigma_{xx1}^T}{G_1}\right),\quad g_{2,1}=\left(\frac{\sigma_{yy1}^T+\sigma_{zz1}^T}{G_1 I_{P1}}\right)A_1,\quad g_{3,1}=\frac{\rho_1}{G_1},\quad P_1=\frac{g_{2,1}}{g_{1,1}},\quad F_1=\frac{g_{3,1}}{g_{1,1}}. \quad (22)$$

$$g_{1,2}=\left(-1-\frac{\sigma_{xx2}^T}{G_2}\right),\quad g_{2,2}=\left(\frac{\sigma_{yy2}^T+\sigma_{zz2}^T}{G_2 I_{P2}}\right)A_2,\quad g_{3,2}=\frac{\rho_2}{G_2},\quad P_2=\frac{g_{2,2}}{g_{1,2}},\quad F_2=\frac{g_{3,2}}{g_{1,2}} \quad (23)$$

The separation variable method given by Eq. (24) is used to obtain the closed-form solutions for the rod segments in which $\omega$is the rod natural frequency.

$$\phi_1(x,t)=\theta_1(x)e^{i\omega t},\phi_2(x,t)=\theta_2(x)e^{i\omega t}. \quad (24)$$

By substituting Eq. (24) into Eqs. (20) and (21), the equations of motion for both segments of the cracked rod are obtained as

$$\frac{\partial^2\theta_1}{\partial x^2}+(P_1-\omega^2F_1)\theta_1=0. \quad (25)$$

$$\frac{\partial^2\theta_2}{\partial x^2}+(P_2-\omega^2F_2)\theta_2=0. \quad (26)$$

The closed form solutions for Eqs. (25) and (26) are presented as following.

$$\theta_1(x)=A_1\sin(\beta_1 x)+A_2\cos(\beta_1 x). \quad (27)$$

$$\theta_2(x)=A_3\,sin(\beta_2 x)+A_4\,cos(\beta_2 x). \quad (28)$$

$$\beta_1=\sqrt{(P_1-\omega^2F_1)},\beta_2=\sqrt{(P_2-\omega^2F_2)}. \quad (29)$$

Focusing on the Eqs. (27) and (28), it will be seen that there are four constants to complete the solutions. So, four boundary conditions are required to obtain the torsional natural frequencies but there are only two boundary conditions for a rod. Two other conditions can be derived from the crack location. The conditions are known as compatibility equations and presented as follows[21, 31].

Jump in twisting angle: $$\Delta\theta=\theta_2(b)-\theta_1(b)=C_c\left.\frac{\partial\theta_1(x)}{\partial x}\right|_{x=b}. \quad (30)$$

Continuity of the twisting moment:

$$G_1I_{P1}\frac{\partial\theta_1(b)}{\partial x}=G_2I_{P2}\frac{\partial\theta_2(b)}{\partial x}. \quad (31)$$

The boundary conditions have already been determined by Eq. (16) for the fixed and free ends of the rod as

Fixed end: $\theta(x)=0$, Free end: $\frac{\partial\theta(x)}{\partial x}=0$. (32)

The constant C_c which represents the crack severity can be related to the crack depth ratio and material properties, and it can be determined as[20, 21]

$$C_c=C\times G\times I_P,C=\frac{4}{\pi R^3G}\times I(a/R). \quad (33)$$

The expression C which is the local flexibility or compliance relates with dimensionless compliance $I(a/R)$ as shown in Eq. (27). The dimensionless compliance $I(a/R)$ can be obtained using crack depth a and rod radius R by the following relation in which $\xi=(1-a/R)$[20].

$$I(a/R)=0.035\xi^{-4}+0.01\xi+0.029\xi^2+0.0086\xi^3+0.0044\xi^4+0.0025\xi^6+0.0017\xi^7+0.008\xi^8-0.029. \quad (34)$$

Finally, the frequency ratio (FR) between the cracked (ω_{cr}) and non-cracked (ω_{non}) torsional frequencies of a cracked rod can be obtained as

$$FR=\frac{\omega_{cr}}{\omega_{non}}. \quad (35)$$

3. Results and discussions

3.1. Material properties

The material properties of the dissimilar rods that have been welded by the friction welding method are tabulated in Table 1. The first rod material shown in Fig. 1 (left rod), is chosen to be duplex stainless steel SAF 2507 and the second rod (right rod) is made up of AISI type 304 stainless steel.

3.2. Benchmark results

In the friction rotary welding, the weld remains in the solid-state, avoiding many of the defects associated with melting and solidification during fusion welding, such as pores and solidification cracks. The distortion of the welded component is also reduced. Friction rotary welding is widely implemented across the manufacturing sector and has been used for numerous applications, including turbine shafts, automotive parts including steel truck axels and casings, monel-to-steel marine fittings, piston rods, copper-aluminium electrical connections, and cutting tools.

The process is easily automated, and it is not dependent on human influence, which results in very low defect rates such as cracks. But, it does not mean that the cracks cannot be generated on the rods. So, a crack or more can be generated on the rod especially at the contact zone, during or after the welding process.If the parts created by friction rotary welding consist of a crack or more, the serious operational problems may occurbecause most of these parts are applied in high temperatures such as piston rod or turbine shafts. In this study, the presence of a crack at the contact zone is considered and its effect is studied. Also, the three-dimensional thermal stresses generated by high temperatures on the rod are considered. The main purpose of this study is to determine how much the crack and three-dimensional thermal stresses can alter the torsional frequencies of a rod composed of two frictionally-welded parts.

In the present study, linear torsional frequencies of a rod composed of two welded rods for cracked and non-cracked cases with clamped-clamped (C-C) and clamped-free (C-F) boundary conditions in a thermal environment are investigated. Thermal stresses are exposed from three mutually directions and consequently, their effect is not negligible. One of the aims of this investigation is to show whether the thermal stresses effects can be neglected or their effect must be taken into account. At the same time, the crack effect on the torsional frequencies must also be examined. Effects of thermal stresses and crack will be significant if they both are simultaneously applied to the rod. For this study, it has been assumed that the geometries of both segments of the rod such as diameter and length are the same so that it can be written that $d = d_1 = d_2 = 2R_1 = 2R_2$ or$A = A_1 = A_2$ and $L_1 = L_2$.

The linear torsional frequencies and frequency ratios of the cracked and non-cracked C-Cand C-Frodsat room temperatureand higher are presented in Table 2 and Table3, respectively. According to the results of Table 2, a decrease in the torsional frequencies of the C-C rod occurs when temperature increases. The crack depth ratio effects $(a\,/R)$ on the frequencies of C-C rods are shown in Table 2.

According to the results of Table3, if the crack depth and temperature highly increase, the C-F cracked rod will extensively be impressed and its frequencies will fall.

The frequency ratio (FR) for the three first modes of the C-C and C-F rods with various crack depth ratios at different high temperatures are tabulated in Tales 2 and 3. As it is obvious, increasing the crack depth ratio and crack severity lead to a decrease in the frequency ratio at any temperature. It means that the frequencies of the cracked rod reduce with increasing the crack depth ratio. Another parameter that alters the frequency ratio is temperature change. The frequency ratio for all modes of the cracked C-C and C-F rods decreases by an increase in temperature for any crack severity. The frequency ratio of the cracked C-F rod is highly impressed by high temperatures and high crack severity values.

Table 1. Geometries and properties of duplex stainless steel SAF 2507 and AISI type 304 stainless steel.

Duplex stainless steel	$\rho_1\ (kg/m^3)$	$R_1(mm)$	$L_1(mm)$	$E_1\ (GPa)$	ν_1	$\alpha_1(1/K)$
SAF 2507	7800	6	25	200	0.3	14×10^{-6}
AISI type 304	$\rho_2\ (kg/m^3)$	$R_2(mm)$	$L_2(mm)$	$E_2\ (GPa)$	ν_2	$\alpha_2\ (1/K)$
stainless steel	8000	6	25	195	0.29	17×10^{-6}

Table 2. First three torsional frequencies and frequency ratios of a cracked C-C rod with different crack depth ratios (a/R) for different temperature changes. ($L = 50\ mm$, $d = 12\ mm$, and $b = L_1 = 25\ mm$).

a/R	ΔT	ω_1(rad/s)	ω_2(rad/s)	ω_3(rad/s)	FR_1	FR_2	FR_3
Non	0	195194.52	390405.20	585583.58	1	1	1
Cracked	40	189039.14	387054.89	583003.27	1	1	1
	80	182675.64	383675.58	580411.40	1	1	1
	120	176081.45	380266.51	577807.79	1	1	1
	160	169229.60	376826.85	575192.30	1	1	1
	200	162087.41	373355.77	572564.75	1	1	1
	300	142671.44	364534.69	565942.05	1	1	1
1/6	0	195194.26	388621.30	585576.71	0.9999986	0.9954306	0.9999882
	40	189038.78	385259.52	582996.02	0.9999981	0.9953614	0.9999875
	80	182675.15	381868.42	580403.76	0.9999973	0.9952898	0.9999860
	120	176080.81	378447.20	577799.75	0.9999963	0.995215	0.9999860
	160	169228.77	374995.04	575183.84	0.9999951	0.9951388	0.9999852
	200	162086.36	371511.09	572555.86	0.9999935	0.9950591	0.9999844
	300	142669.63	362656.07	565932.02	0.9999873	0.9948465	0.9999822
2/6	0	195193.08	380586.70	585544.89	0.9999926	0.9748504	0.9999339
	40	189037.11	377171.64	582962.46	0.9999892	0.9744655	0.9999300
	80	182672.89	373725.71	580368.38	0.9999849	0.9740669	0.9999258
	120	176077.83	370248.03	577762.50	0.9999794	0.9736540	0.9999216
	160	169224.93	366737.72	575144.66	0.9999724	0.9732260	0.9999171
	200	162081.50	363193.83	572514.69	0.9999635	0.9727821	0.9999125
	300	142661.25	354180.54	565885.57	0.9999285	0.9715962	0.9999002
3/6	0	195188.17	351493.27	585412.54	0.9999674	0.9003293	0.9997079
	40	189030.17	347860.74	582822.84	0.9999525	0.8987374	0.9996905
	80	182663.47	344190.45	580221.25	0.9999333	0.8970870	0.9996723
	120	176065.42	340481.18	577607.60	0.9999089	0.8953751	0.9996535
	160	169208.94	336731.65	574981.74	0.9998779	0.8935978	0.9996339
	200	162061.23	332940.50	572343.48	0.9998384	0.8917513	0.9996135
	300	142626.33	323270.92	565692.49	0.9996838	0.8868042	0.9995590
4/6	0	195158.30	271226.74	584633.11	0.9998144	0.6947313	0.9983768
	40	188988.01	266712.47	582001.89	0.9997295	0.6890817	0.9982823
	80	182606.26	262122.61	579357.51	0.9996202	0.6831881	0.9981842
	120	175990.06	257453.10	576699.78	0.9994809	0.6770333	0.9980823
	160	169111.85	252699.56	574028.52	0.9993042	0.6705986	0.9979767
	200	161938.25	247857.15	571343.55	0.9990797	0.6638631	0.9978671
	300	142414.65	235326.16	564569.85	0.9982001	0.6455521	0.9975753
5/6	0	194644.39	202878.93	580480.07	0.9971816	0.5196624	0.9912847
	40	188281.42	197147.76	577730.41	0.9959917	0.5093534	0.9909556
	80	181674.46	191265.16	574967.46	0.9945193	0.4985075	0.9906205
	120	174798.66	185214.02	572191.03	0.9927147	0.4870637	0.9902791
	160	167623.61	178974.76	569400.93	0.9905099	0.4749522	0.9899314
	200	160111.53	172524.70	566596.98	0.9878097	0.4620919	0.9895771
	300	139509.25	155289.20	559525.14	0.9778358	0.4259929	0.9886615
5.5/6	0	193342.42	197556.84	579455.86	0.9905115	0.5060302	0.9895357
	40	186768.97	191843.15	576700.74	0.9879910	0.4956484	0.9891895
	80	179955.06	185954.46	573932.41	0.9851070	0.4846658	0.9888372
	120	172872.45	179873.43	571150.65	0.9817754	0.4730193	0.9884786
	160	165486.73	173579.72	568355.28	0.9778828	0.4606352	0.9881135
	200	157755.41	167049.25	565546.09	0.9732736	0.4474264	0.9877417
	300	136524.28	149480.62	558461.29	0.9569138	0.4100587	0.9867817

Table 3. First three torsional frequencies and frequency ratios of a cracked C-F rod with different crack depth ratios (a/R) for different temperature changes. ($L = 50\ mm$, $d = 12\ mm$, and $b = L_1 = 25\ mm$).

a/R	ΔT	ω_1(rad/s)	ω_2(rad/s)	ω_3(rad/s)	FR_1	FR_2	FR_3
Non Cracked	0	97479.34	292917.64	487876.88	1	1	1
	40	84345.64	288733.65	484987.23	1	1	1
	80	68745.37	284488.23	482080.27	1	1	1
	120	48347.09	280178.56	479155.69	1	1	1
	160	…	275801.64	476213.17	…	1	1
	200	…	271354.21	473252.37	…	1	1
	300	…	259903.24	465768.12	…	1	1
1/6	0	97252.12	292279.91	486664.89	0.9976690	0.9978228	0.9975157
	40	84080.70	288090.79	483767.44	0.9968588	0.9977735	0.9974849
	80	68417.30	283839.93	480852.55	0.9952277	0.9977211	0.9974532
	120	47875.51	279524.52	477919.90	0.9902459	0.9976656	0.9974209
	160	…	275141.52	474969.16	…	0.9976065	0.9973877
	200	…	270687.63	472000.00	…	0.9975435	0.9973537
	300	…	259218.68	464494.14	…	0.9973661	0.9972647
2/6	0	96213.86	289364.27	481157.98	0.98701797	0.9878690	0.9862282
	40	82867.48	285151.05	478224.94	0.98247497	0.9875920	0.9860567
	80	66908.18	280874.72	475273.82	0.97327544	0.9872982	0.9858810
	120	45674.52	276532.35	472304.29	0.94472118	0.9869861	0.9857011
	160	…	272120.79	469315.99	…	0.9866540	0.9855166
	200	…	267636.61	466308.57	…	0.9862998	0.9853274
	300	…	256083.21	458703.89	…	0.9853021	0.9848331
3/6	0	92130.39	278059.74	460980.51	0.94512735	0.9492761	0.9448705
	40	78050.99	273742.92	457914.98	0.92537077	0.9480811	0.9441794
	80	60792.09	269357.03	454828.84	0.88430814	0.9468125	0.9434711
	120	36044.05	264898.66	451721.67	0.74552677	0.9454637	0.9427450
	160	…	260364.08	448593.04	…	0.9440265	0.9420004
	200	…	255749.22	445442.49	…	0.9424921	0.9412366
	300	…	243830.75	437467.13	…	0.9381597	0.9392380
4/6	0	74092.12	239006.93	413101.55	0.76008024	0.8159526	0.8467332
	40	55476.70	234182.63	409707.60	0.6577305	0.8110680	0.8447801
	80	25798.19	229257.04	406285.33	0.37527167	0.8058577	0.8427752
	120	…	224223.48	402834.03	…	0.8002877	0.8407163
	160	…	219074.50	399352.94	…	0.7943190	0.8386012
	200	…	213801.77	395841.28	…	0.7879065	0.8364274
	300	…	200013.68	386922.91	…	0.7695697	0.8307200
5/6	0	25815.69	200921.88	388079.04	0.26483243	0.6859330	0.7954446
	40	…	195301.17	384507.16	…	0.6764059	0.7928191
	80	…	189513.84	380901.79	…	0.6661570	0.7901210
	120	…	183544.12	377261.96	…	0.6550969	0.7873473
	160	…	177373.60	373586.68	…	0.6431201	0.7844946
	200	…	170980.54	369874.87	…	0.6301009	0.7815594
	300	…	153839.97	360428.16	…	0.5919124	0.7738360
5.5/6	0	6633.14	197544.66	386367.72	0.06804662	0.6744034	0.7919369
	40	…	191832.46	382783.77	…	0.6643924	0.7892656
	80	…	185944.87	379165.93	…	0.6536118	0.7865203
	120	…	179864.67	375513.24	…	0.6419644	0.7836977
	160	…	173571.60	371824.67	…	0.6293349	0.7807946
	200	…	167041.62	368099.15	…	0.6155851	0.7778073
	300	…	149473.78	358616.04	…	0.5751131	0.7699454

Fig. 2 represents how the torsional frequencies of the C-C and C-F rods with and without crack vary with temperature changes. For the case of the cracked rods, frequencies of all modes are more impressed by temperature changes. Generally, all mode frequencies of the non-cracked rods are higher than the cracked rods at any temperature and with any boundary conditions. An increase in the temperature leads to a decrease in all mode torsional frequencies of the C-C and C-F rods for any crack depth ratio or crack severity.

This is because the structures become softer, weaker, and more ductile at high temperatures which result in lower stiffness and lower frequencies. Therefore, it can be stated that high temperatures cause a reduction in axial rigidity, bending stiffness, and torsional rigidity.Mehta and Kumar [33] have already found that the torsional characteristics, such as torsional rigidity and damping are temperature-dependent.

It is worth mentioning that the effect of the crack with high crack severity (crack severity directly changes with changes of crack depth ratio) becomes very dangerous when the cracked rod is exposed to high temperatures simultaneously. For this reason, such cracked rods must never vibrate at high temperatures because the failure of the rod or structure will soon occur. It is obvious that the

C-F rod is more impressed by the crack and temperature changes than the C-C rod. It implies how the boundary condition can play an important role in the dynamics of structures. Increasing the crack depth ratio causes an increase in the crack severity and additional flexibility of the rods. This leads to a reduction of the torsional frequencies of the C-C and C-F rods at any temperature. As the vibration mode increases, the thermal and crack effects on the rods with any boundary condition increases. It means that the fundamental frequency is more impressed by the crack and thermal changes than the second and third modes. In Fig 2, the case of "Non-Cr" denotes the non-cracked rod case. The lowest torsional frequencies for both C-C and C-F rods at any mode are obtained when the value of crack depth ratio is low and temperature is high and in such cases, the frequencies approach minimum values. As it is seen, the first mode of the C-F does not have a real value, and it has become imaginary. This is due to the extraordinary flexibility induced to the C-F rod by a crack at elevated temperatures. It is worth mentioning that the torsional frequencies increase at temperatures lower than room temperature for any crack severity value and for any boundary condition as already proved by Abdullah et al. [15].

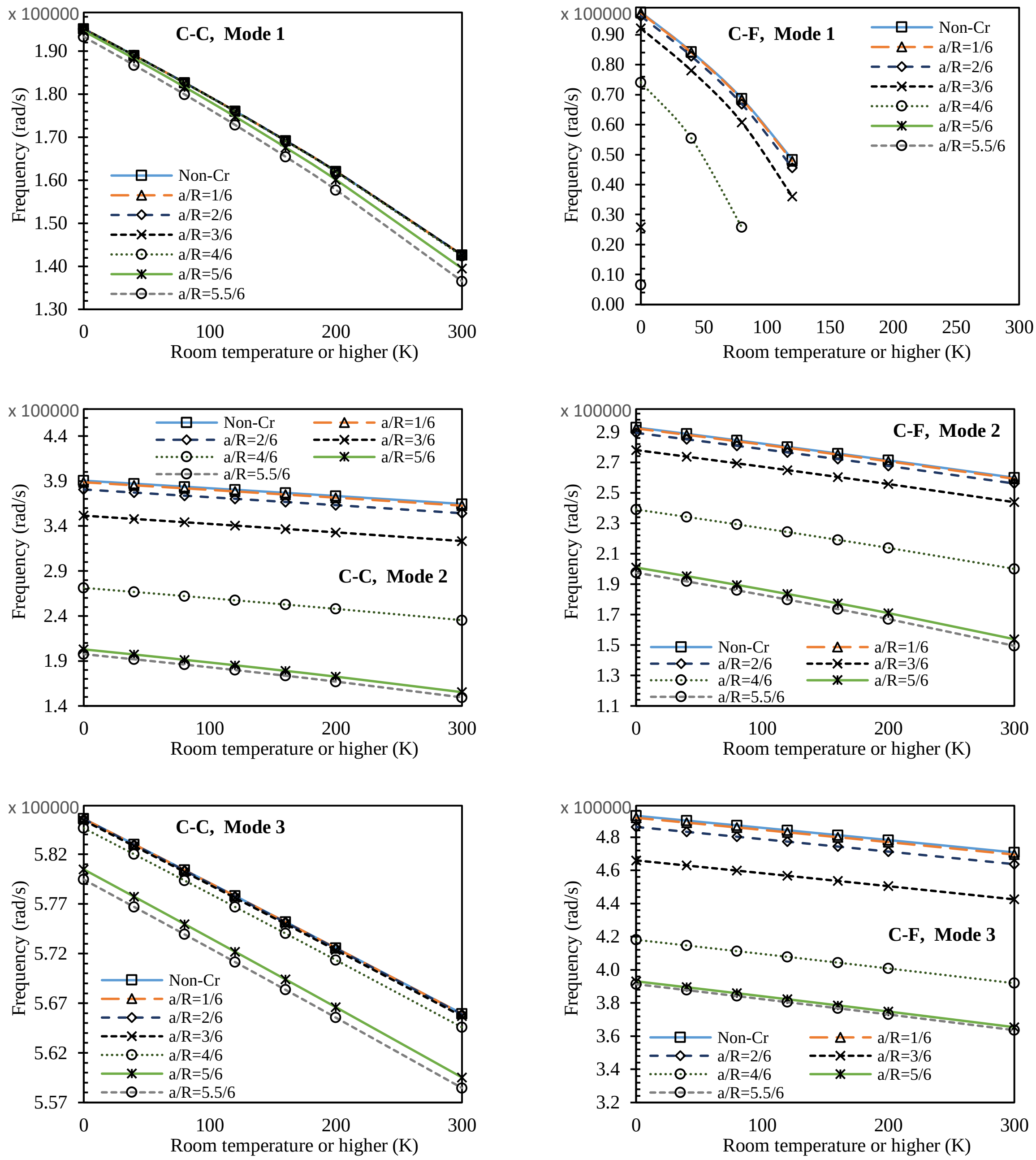

Figure 2. Variation of first three frequencies of cracked C-C and C-F rods versus room temperature or higher for different crack depth ratios. ($L = 50\ mm$, $d = 12\ mm$, and $b = L_1 = 25\ mm$).

The comparative parameter that is known as "difference percent" is a very important and usefulparameter to determine what parameters cause the temperature influence on the torsional frequencies to increases or decrease.The value of the difference percent is dependent on the other parameter valuesC_c, b,L, and R.

$$Difference\ percent = \frac{|frequency_T - frequency_{T_{room}}|}{frequency_{T_{room}}} \times 100. \quad (36)$$

Here, $frequency_T$ is the frequency at temperature$T$, and $frequency_{T_{room}}$ is the frequency at room temperature.

According to Fig. 3,it can be observed that increasing the crack depth ratio a/R, consequently increasing the crack severity, leads to an increase in different percent of the rods with any boundary conditions for any vibration mode. This exactly means that the torsional frequencies will be more impressed by temperature changes when the crack is severe or intensive. If the crack severity is low value, all mode frequencies will not be highly sensitive to temperature changes. From the presented curves of Fig. 3, it is seen that the lower modes decrease more than the higher modes due to the temperature changes. As, reduction of the first mode is more than the second and third modes, and the second mode reduction is more than the third mode. It can be noted that the effect of thermal stresses on the torsional frequencies of the cracked rods of C-C and C-F rods cannot be negligible especially at elevated temperatures and high values of the crack severities, and this effect should be taken into account for rod design. The difference percent or effect of temperature changes on the frequencies of the C-F rod is more than the C-C rod because the C-C rod is stiffer than the C-F rod because of possessing two fixed ends.

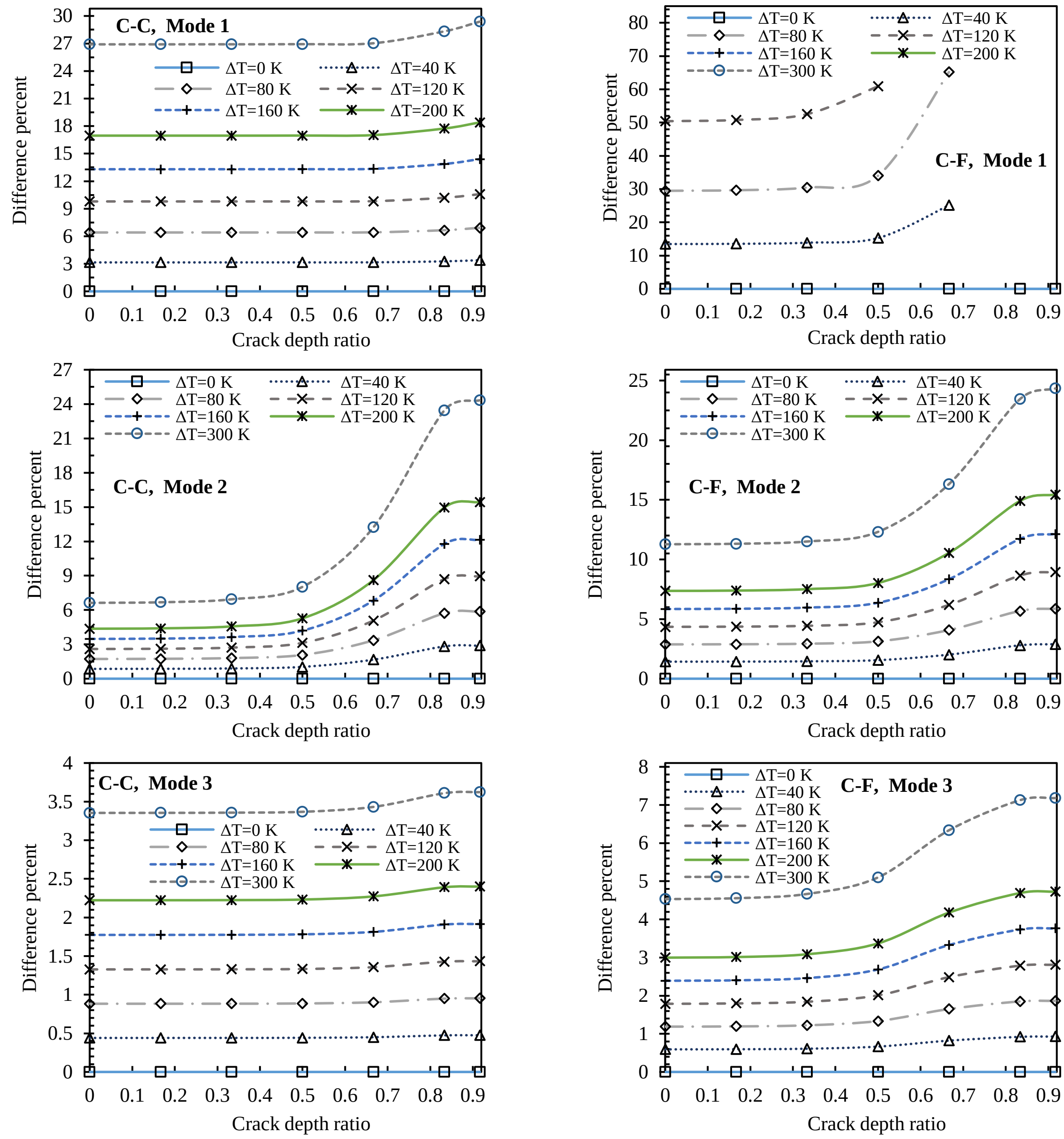

Figure 3. Difference percent of first three modes of C-C and C-F rods versus crack depth ratio at room temperature or higher. ($L = 50\ mm$, $d = 12\ mm$, and $b = L_1 = 25\ mm$).

4. Conclusions

The following conclusions are made according to the obtained results throughout this study.

- The linear torsional frequencies of non-cracked and cracked rods decline when the temperature is higher than room temperature for any boundary conditions, any crack severity, and any crack depth ratio.
- Increasing the crack depth leads to an increase in the crack severity and a decrease in all torsion frequency modes of the rod composed of two welded parts for any boundary condition at any temperature.
- Lower modes are more impressed by temperature and crack depth changes than higher modes.
- The frequency ratio of the C-C and C-F rods decreases with increasing temperature and crack depth ratio for all vibration modes.
- The difference percent increases with increasing the crack severity. The influence of the temperature on the frequencies becomes low when the crack is not deep. Increasing the difference percent of the C-F rod is much higher than that of the C-C rod for any crack depth especially for the first mode.

Acknowledgments

The authors are grateful to the University of Salahaddin-Erbil for supporting this work.

References

[1] C. Rhodes, M. Mahoney, W. Bingel, R. Spurling, C. Bampton, “Effects of friction stir welding on microstructure of 7075 aluminum”. Scripta materialia, Vol. 36, No. 1, 1997, 69-75.

[2] H. Seli, M. Awang, A.I.M. Ismail, E. Rachman, Z.A. Ahmad, “Evaluation of properties and FEM model of the friction welded mild steel-Al6061-alumina”. Materials Research, Vol. 16, No. 2, 2013, 453-467.

[3] R.S. Mishra, Z. Ma, “Friction stir welding and processing”. Materials science and engineering: R: reports, Vol. 50, No. 1-2, 2005, 1-78.

[4] N.R.J. Hynes, P.S. Velu, “Simulation of friction welding of alumina and steel with aluminum interlayer”. The International Journal of Advanced Manufacturing Technology, Vol. 93, No. 1, 2017, 121-127.

[5] N.R.J. Hynes, R. Tharmaraj, “Thermal Model for Heat Flow in Friction Stud Welding”. J Therm Eng Appl, Vol. 2, No. 2, 2015, 22-27.

[6] G. Irwin, J. Kies, “Fracturing and fracture dynamics”. Welding Journal, Vol. 31, No. 2, 1952, 95-100.

[7] J. Loya, J. López-Puente, R. Zaera, J. Fernández-Sáez, “Free transverse vibrations of cracked nanobeams using a nonlocal elasticity model”. Journal of Applied Physics, Vol. 105, No. 4, 2009, 044309.

[8] Z.P. Baiant, L. Cedolin, “Finite element modeling of crack band propagation”. Journal of Structural Engineering, Vol. 109, No. 1, 1983, 69-92.

[9] T. Chondros, “The continuous crack flexibility model for crack identification”. Fatigue & Fracture of Engineering Materials & Structures, Vol. 24, No. 10, 2001, 643-650.

[10] O. Jun, H. Eun, Y.-Y. Earmme, C.-W. Lee, “Modelling and vibration analysis of a simple rotor with a breathing crack”. Journal of sound and vibration, Vol. 155, No. 2, 1992, 273-290.

[11] T.G. Chondros, A.D. Dimarogonas, J. Yao, “Vibration of a beam with a breathing crack”. Journal of sound and vibration, Vol. 239, No. 1, 2001, 57-67.

[12] S. Nacy, N. Alsahib, F. Mustafa, “Vibration analysis of plates with spot welded stiffeners”. Jordan Journal of Mechanical and Industrial Engineering, Vol. 3, No. 4, 2009, 272-279.

[13] M. Ghadiri, K. Malekzadeh, F.A. Ghasemi, “Free Vibration of an Axially Preloaded Laminated Composite Beam Carrying a Spring-Mass-Damper System with a Non-Ideal Support”. Jordan Journal of Mechanical and Industrial Engineering, Vol. 9, No. 3, 2015,

[14] S.H.H. Kachapi, “Nonlinear Vibration and Frequency Analysis of Functionally Graded-Piezoelectric Cylindrical Nano-shell with Surface Elasticity”. Jordan Journal of Mechanical and Industrial Engineering, Vol. 12, No. 4, 2018,

[15] S.S. Abdullah, S. Hosseini-Hashemi, N.A. Hussein, R. Nazemnezhad, “Temperature change effect on torsional vibration of nanorods embedded in an elastic medium using Rayleigh–Ritz method”. Journal of the Brazilian Society of Mechanical Sciences and Engineering, Vol. 42, No. 11, 2020, 1-20.

[16] S.S. Abdullah, S.H. Hashemi, N.A. Hussein, R. Nazemnezhad, “Three-Dimensional Thermal Stress Effects on Nonlinear Torsional Vibration of Carbon Nanotubes Embedded in an Elastic Medium”. Nanoscale and Microscale Thermophysical Engineering, Vol. 25, No. 3-4, 2021, 1-28.

[17] X. Zhu, L. Li, “Longitudinal and torsional vibrations of size-dependent rods via nonlocal integral elasticity”. International Journal of Mechanical Sciences, Vol. 133, No., 2017, 639-650.

[18] L. Li, Y. Hu, “Torsional vibration of bi-directional functionally graded nanotubes based on nonlocal elasticity theory”. Composite Structures, Vol. 172, No., 2017, 242-250.

[19] R. Barretta, S.A. Faghidian, R. Luciano, C. Medaglia, R. Penna, “Stress-driven two-phase integral elasticity for torsion of nano-beams”. Composites Part B: Engineering, Vol. 145, No., 2018, 62-69.

[20] A. Dimarogonas, G. Massouros, “Torsional vibration of a shaft with a circumferential crack”. Engineering Fracture Mechanics, Vol. 15, No. 3-4, 1981, 439-444.

[21] T. Chondros, A. Dimarogonas, “Dynamic sensitivity of structures to cracks”. Journal of Vibration and Acoustics, Vol. 111, No. 3, 1989, 251-256.

[22] P. Rizos, N. Aspragathos, A. Dimarogonas, “Identification of crack location and magnitude in a cantilever beam from the vibration modes”. Journal of sound and vibration, Vol. 138, No. 3, 1990, 381-388.

[23] J. Loya, J.a. Aranda-Ruiz, J. Fernández-Sáez, “Torsion of cracked nanorods using a nonlocal elasticity model”. Journal of Physics D: Applied Physics, Vol. 47, No. 11, 2014, 115304.

[24] M. Marin, “On the domain of influence in thermoelasticity of bodies with voids”. Archivum Mathematicum, Vol. 33, No. 3, 1997, 301-308.

[25] M. Marin, “A temporally evolutionary equation in elasticity of micropolar bodies with voids”. Bull Ser Appl Math Phys, Vol. 60, No. 3-4, 1998, 3-12.

[26] S. Amini, M. Amiri, “Study of ultrasonic vibrations’ effect on friction stir welding”. The International Journal of Advanced Manufacturing Technology, Vol. 73, No. 1, 2014, 127-135.

[27] J. Reddy, P. Mahaffey, “Generalized beam theories accounting for von Kármán nonlinear strains with application to buckling”. Journal of Coupled Systems and Multiscale Dynamics, Vol. 1, No. 1, 2013, 120-134.

[28] J. Reddy, S. El-Borgi, J. Romanoff, “Non-linear analysis of functionally graded microbeams using Eringen′ s non-local differential model”. International Journal of Non-Linear Mechanics, Vol. 67, No., 2014, 308-318.

[29] J.N. Reddy. Mechanics of laminated composite plates and shells: theory and analysis. 2nd ed. New York: CRC press; 2003.

[30] J.R. Vinson, R.L. Sierakowski. The behavior of structures composed of composite materials. 2nd ed. Netherlands: Springer; 2006.

[31] S.S. Abdullah, S.H. Hashemi, N.A. Hussein, R. Nazemnezhad, "Effect of three-dimensional thermal stresses on torsional vibration of cracked nanorods surrounded by an elastic medium". Advances in nano research, Vol. 11, No. 3, 2021, 251-269.

[32] G. Praveen, J. Reddy, "Nonlinear transient thermoelastic analysis of functionally graded ceramic-metal plates". International Journal of Solids and Structures, Vol. 35, No. 33, 1998, 4457-4476.

[33] V. Mehta, S. Kumar, "Temperature dependent torsional properties of high performance fibres and their relevance to compressive strength". Journal of materials science, Vol. 29, No. 14, 1994, 3658-3664.